VIII- Ⅱ -1.　　Project Research

Project 1

PR1　Fundamental and Developmental Research on Physical and Chemical Characteristics of Actinides

H. Yamana

Research Reactor Institute, Kyoto University

1. Objectives and Allotted Research Subjects

Studies on actinide elements are categorized into two subjects, that is, a) engineering studies with the standpoint of nuclear fuel cycle, and b) fundamental studies with the standpoint of physics and chemistry. National laboratories are directed to the engineering vocation, while university laboratories are permissible to concentrate on the basic research. The principal objective of the present project research is to provide scientific and technological basis of physics and chemistry of actinide elements. Thus it covers various experimental studies of actinides and transactinides, on nuclear properties, radiochemical and other chemical properties, process chemistry, and material properties, and so on. Allotted research subjects are as the followings.

ARS-1　Study on neutron capture cross sections of long-lived nuclides by activation method (S. Nakamura *et al.*)

ARS-2　Isotope production and application by using actinides (S. Shibata *et al.*)

ARS-3　Spectroelectrochemical analysis of actinide ions in molten salts (A. Uehara *et al.*)

ARS-4　Study on chemical isotope effect of actinides and fission product elements (T. Fujii *et al.*).

ARS-5　Thermodynamic study of actinide complexes in aqueous solution (T. Sasaki *et al.*).

ARS-6　Fundamental study on solid-state properties of perovskite type oxides (S. Yamanaka *et al.*).

ARS-7　Assessment study on chemical properties of actinides in molten salts (M. Myochin *et al.*).

ARS-8　Electrochemical study of uranium in pyrochemical reprocessing system (Y. Sakamura *et al.*).

ARS-9　Basic study for "atom at a time chemistry" of heavy actinide and trans-actinide elements (A. Shinohara, *et al.*)

ARS-10　Study on coordination chemistry of actinide elements (Y. Ikeda *et al.*).

2. Main Results and Contents

Nuclear physical properties of TRUs were investigated in the study, ARS-1. By activation method using KUR, the thermal-neutron capture cross section of ^{237}Np was newly evaluated. Adsorption properties of FPs were investigated in the study, ARS-2. Adsorption rates of 11 FPs on a soil were investigated. ARS-3, ARS-7, ARS-8, and ARS-10 studied the chemical behavior of actinides in molten salt and ionic liquid systems, the results of which are to be dedicated to the development of reprocessing technique. ARS-3 studied electrochemical behavior of the $Nd^{3+}|Nd^{2+}$ and $Nd^{2+}|Nd$ couples in molten $LiCl$-$CaCl_2$ eutectic. Electrochemical separation of Nd was performed by disproportionation reaction of Nd^{2+} prepared from Nd^{3+}. In ARS-7, the UO_2^{2+}/UO_2^+ redox potential in Li_2MoO_4–Na_2MoO_4 eutectic melt was evaluated by using the spectrophotometric technique. It was determined to be $E°=0.277$. ARS-8 studied a possibility to apply chronopotentiometry for understanding anodic behavior of U-Zr alloy in LiCl-KCl melt. The diffusion coefficient of UCl3 experimentally evaluated agreed with the value of the porous Zr layer assumed in the anode model. ARS-10 studied electrochemical properties of uranyl chloride complexes in an ionic liquid. The chemical structure and electrochemical behavior of uranyl(VI) species, $(EMI)_2UO_2Cl_4$, in the mixture of EMICl and $EMIBF_4$ (EMI = 1-ethyl-3-methylimidazoliun) were examined. ARS-4 studied the coordination circumstance of UO_2^{2+} in concentrated nitrate solution by Raman spectrometry. The symmetric ν_1 vibration of O=U=O was clearly found. In ARS-5, complexation of Th(IV) with fumic substances was investigated. The apparent formation constant was determined to be >20. ARS-6 studied thermal expansion of calcium series perovskite-type oxides. The average thermal expansion coefficients for $CaTiO_3$, $CaZrO_3$, and $CaHfO_3$ were determined. In ARS-9, for understanding Sg chemistry, solvent extraction behavior of tungsten (W) was investigated. The extracted species of W was assigned to be $WO_2Cl_3^-$.

3. Summaries of the achievements

In this research, by using various unique facilities of KURRI for actinide research, new and characteristic chemical and nuclear physical data were obtained. These new information encompass solid chemistry, molten salt and solution chemistry, as well as nuclear reactions of actinides. The results are useful either for scientific purpose or for technological purpose for actinide management in the nuclear fuel cycle.

PR1-1   Measurements of Neutron Capture Cross Sections for Radioactive Nuclei

S.Nakamura, F.Kitatani, H.Harada
T.Fujii[1] and H.Yamana[1]

Japan Atomic Energy Agency
[1]*Research Reactor Institute, Kyoto University*

INTRODUCTION: As a part of the research projects, a series of cross-section measurements has been carried out for minor actinides to obtain basic data for studies on nuclear-fuel cycles and nuclear transmutation. Neptunium-237 is one of important isotopes because it contributes to the long-term radiotoxicity of nuclear wastes. However, there still exist large discrepancies among reported data of the thermal-neutron capture cross section. Then, the present work reports the measurement for the thermal-neutron capture cross-section of ^{237}Np.

EXPERIMENTS: A standardized solution of ^{237}Np was used for irradiation samples. Sufficient amounts of solutions (200Bq) were dropped onto filter papers. After drying the filters, they were packed into vinyl bags. Sets of Au/Al alloy wire and a Co foil were used to monitor neutron fluxes at an irradiation position. The ^{237}Np sample was irradiated together with the monitor set for 600 sec in the pneumatic tube (Pn-2) of the KUR. Another ^{237}Np sample and the monitor set were rapped with a Gd foil, the thickness of which was selected in 25μm to set the cut-off energy at 0.13eV. Since ^{237}Np has the huge first resonances at 0.489eV, the present cut-off energy shall be appropriate to eliminate the effect from the first resonance. The ^{237}Np sample shielded with the Gd foil was irradiated for 300 sec in Pn-2. After the irradiations, induced activities of samples were measured with a high purity Ge detector. **Fig. 1** shows an example of γ-ray spectra obtained from the measurements of the irradiated ^{237}Np sample. The measurement time was 20 min.
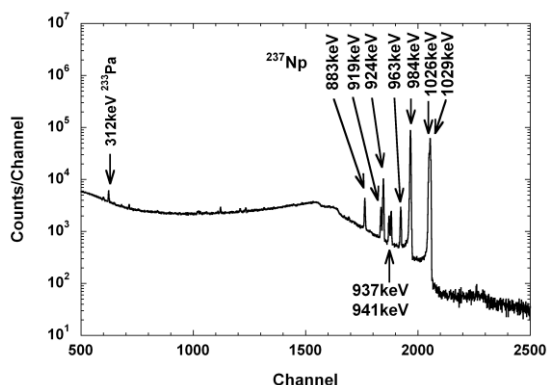
were repeated twice to confirm the reproducibility of reaction rates of the samples.

ANALYSES AND RESULTS: The spectral data taken from the γ-ray measurements were analyzed to obtain neutron fluxes, induced activities and reaction rates. The thermal neutron flux was derived from the induced activities of the monitors on the basis of the Westcott's convention [1], and obtained as $(4.4\pm0.1)\times10^{12}$ n/cm^{2}s at the irradiation position of Pn-2 in 1-MW reactor operation. The epi-thermal index[1] was 0.039.

The reaction rates of ^{237}Np samples were calculated with γ-ray yields, efficiencies, decay data and γ-ray emission probabilities. Though the γ-ray emission probability for 984-keV emitted from ^{238}Np was recently measured, there are still discrepancies among reported data: 41.6$\pm$0.9% by Harada[2], 38.5$\pm$0.4% by Singh[3], and 38.7$\pm$0.4 % by Woods[4]. The value (41.6%) might be overestimated. This point should be remained as a problem. While the γ-ray emission probability for 312-keV emitted from ^{233}Pa, the recent data are in good agreement with each other: 25.2$\pm$0.5% by Harada[2], 25.17$\pm$0.13% by Rengan[5], and 25.19$\pm$0.21% by Chukreev[6]. Reviewing these reported data, the values of 25.2% for 312-keV and 38.5% for 984-keV were used in this work.

The thermal-neutron capture cross section of ^{237}Np was derived from the results of ^{237}Np reaction rates and neutron fluxes using the Westcott's convention. The present work finds the value of 183$\pm$7 b, which is in good agreement with the evaluated data in JENDL-4.0 (178 b) and JEFF-3.1 (181 b) within the limits of error, but about 13% larger than that in ENDF/B-VII (162 b).

REFERENCES:
[1]C.H.Westcott *et al.*, "*Proc.2nd Int.Conf.Peaceful Use of Atomic Energy, Geneva*", United Nations, New York,**16**(1958)70.
[2]H.Harada *et al.*,J.Nucl.Sci.Technol.,**43** (2006) 1289.
[3]B.Singh and J.K.Tuli, Nuclear Data Sheet, **105** (2005) 109.
[4]S.A.Woods *et al.*, Appl. Radiat. Isot., **52** (2000) 475.
[5]K.Rengan, D.Devries *et al.*, Nucl. Instr. Meth. **A556**, (2006) 612.
[6]F.E.Chukreev, V.E.Makarenko *et al.*, Nuclear Data Sheet, **97** (2002) 129.

Fig.1. An example of γ-ray spectra obtained from the measurement of the irradiated ^{237}Np sample.

The γ-ray measurements of the irradiated ^{237}Np samples

Adsorption Rate of Fission Products for Soils

K. Takamiya

Research Reactor Institute, Kyoto University

INTRODUCTION: A severe accident of nuclear reactors results in nuclear core damage, and may cause many kinds of fission products (FPs) to be released to the environment over large area. A part of the released FPs is dispersed by the wind and falls out of the atmosphere. If the FPs fell-down on soils, most of the FPs is deposited on the soil surface, but a part of them moves to surface water. As a result, drinking water, vegetables and others are contaminated with fission products such as ^{131}I and ^{134}Cs. Hence, it is important to study the behavior of FPs in soils.

In the present work, adsorption behavior of FPs in soils has been investigated using a fission multitracer [1, 2]. Tracer isotopes in the multitracer are produced by thermal-neutron-induced fission of ^{235}U using a research reactor. The multitracer contains FPs such as ^{131}I and ^{134}Cs under trace-level concentrations.

EXPERIMENTS: The fission multitracer was prepared by the following procedure. A mixed powder of natural uranium oxide and sodium chloride was irradiated by neutrons using pneumatic irradiation facility (Pn-2) of Kyoto University Research Reactor (KUR). After the neutron irradiation, FPs produced in the mixed powder were separated from the powder by filtration using 0.01 M hydrochloric acid. Pure water was added to the filtrate to adjust the pH of the solution to be 5 to 7.

The prepared multitracer solution (20 mL) was mixed with a Kuroboku-soil (2 g) in a plastic bottle. Five mixed solutions were prepared in this work, and the bottles were shaken once a day. The aging variation of adsorption ratios of FPs to the soils were observed by means of measurements of radio activities in the solution which was separated from soil particles by filtration after 3, 7, 14, 21 and 28 days of the mixing.

RESULTS: Eleven FPs (^{86}Rb, ^{95}Zr, ^{95}Nb, ^{103}Ru, ^{131}I, ^{134}Cs, ^{140}Ba, ^{140}La, ^{141}Ce, ^{144}Ce and ^{147}Nd) were identified in the present work. The observed aging variations of the adsorption ratio of various FPs are shown in Fig. 1. All the adsorption ratios of FPs reach over 80% within 30 days. But the tendency of the aging variation is different among the FPs.

In the case of ^{131}I, the adsorption ratio decreases in first week. And after a week, the ratio increases monotonically. The ratios of ^{95}Zr, ^{95}Nb and ^{103}Ru increase in the first two to three weeks, and then the ratios seem to reach equilibrium state. On the other hand, the ratios of ^{86}Rb, ^{134}Cs, ^{140}Ba, ^{140}La, ^{141}Ce, ^{144}Ce and ^{147}Nd show scarce aging variations.

If an FP is volatile or gaseous, the released amount to the environment becomes larger. Thus, ^{131}I, ^{133}I, ^{134}Cs and ^{137}Cs are the most important FPs in a severe accident. In fact, isotopes of iodine and cesium contaminate the environment and have been detected in drinking water, vegetables etc. over larger areas. Because it needs longer time to adsorb on soils in the case of iodine isotopes, various environmental effects can be expected. On the other hand, isotopes of cesium adsorb on soils rapidly, and scarce migration of the isotopes is expected. But, if the chemical forms of isotopes change, the adsorption behaviors might change. So, information about conditions of soils such as pH, rainfall, moisture content is important for detailed estimation of environmental effects such as migration of FPs.
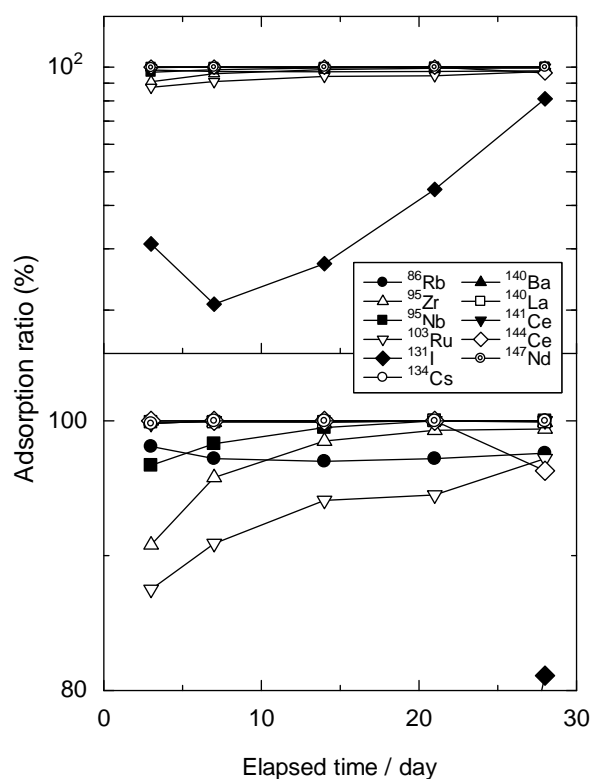

Fig. 1. Aging variations of the adsorption ratio of fission products.

REFERENCES:
[1] K. Takamiya *et al*, J. Nucl. Radio chem. Sci. **1** (2000) 81.
[2] K. Takamiya *et al,* Czech J. Phys. **56** (2006) 399.

PR1-3 Separation of Nd metal by using Disproportionation Reaction of Nd(II) in Molten Chlorides

A. Uehara[1], K. Fukasawa[2], T. Nagai[3], T. Fujii[1] and H. Yamana[1]

[1] *Research Reactor Institute, Kyoto University*
[2] *Graduate school of engineering, Kyoto University*
[3] *Nuclear Fuel Cycle Engineering Lab., Japan Atomic Energy Agency*

INTRODUCTION: The chemical characteristics of lanthanides (Ln) in chloride melts merit further investigation for enhancing the chemical basis of Ln in molten salts and for developing techniques for Ln refining in pyro-electrochemical reprocessing process of spent nuclear fuels [1]. One of the particular interests in relation to the performance of the electrolytic refining of Ln in molten salts is the formation of Ln's divalent states. Neodymium Nd is one of the Lns that have divalent state and its chemical behavior has been investigated in molten LiCl-KCl eutectic [2]. As one of the chemical characteristics of Nd, Nd^{2+} disproportionates into metallic Nd and Nd^{3+} when Nd^{2+} is dissolved in the molten salt [3]. In the present work, electrochemical behavior for the redox of the $Nd^{3+}|Nd^{2+}$ and $Nd^{2+}|Nd$ couples in molten $LiCl$-$CaCl_2$ eutectic were studied, electrochemical separation of Nd was performed by disproportionation reaction of Nd^{2+} prepared from Nd^{3+}.

EXPERIMENTAL: For the cyclic voltammetry experiment of $LiCl$-$CaCl_2$ eutectic system, about 0.1 mol% $NdCl_3$ solutions of molten $LiCl$-$CaCl_2$ (65:35) eutectic was used. Quartz test tubes of 13 mm inner diameter were used for the measurement. A 1.0 mmϕ tungsten rod was used for working electrode and a pyro-graphite carbon rod of 3 mmϕ was used for the counter electrode, both covered with glass sheath. An $Ag|Ag^+$ reference electrode composed with an Ag wire|1 mol% AgCl in a bulk melt|PYREX glass membrane tube was used. Electrochemical measurement system HZ-5000 (Hokuto-Denko Co. Ltd.) was used for the voltammetry measurements. The constant potential electrolysis was performed using Ag wire and $LiCl$-$CaCl_2$ contained in a PYREX glass membrane tube as counter electrode to avoid cyclic redox reaction between tungsten working and counter electrode. After sufficient hours of electrolysis for completing the reduction, sample solution was taken by sampling glass tube having glass filter to separate from deposited materials. All the experiments were carried out in a glove box filled with dry argon whose humidity and oxygen impurity was continuously kept less than 1 ppm.

RESULTS: When the reductive potential to form Nd^{2+} from Nd^{3+} is applied, electrochemical reaction occurs as follows;

$$Nd^{3+} \quad + \quad e^- \quad \rightarrow \quad Nd^{2+} \qquad (1)$$

However, generated Nd^{2+} disproportionates to form Nd^{3+} and metallic Nd chemically,

$$3\,Nd^{2+} \quad \rightleftarrows \quad 2\,Nd^{3+} \quad + \quad Nd \qquad (2)$$
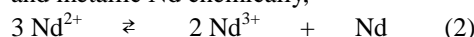
Assuming that the reaction of Eq. (2) proceeds forward direction quantitatively, Nd^{3+} was reduced to form metallic Nd at the potential of Nd^{2+}. Here, number of electron which is necessary to form metallic Nd by the electrolysis is three. Eq. (3) is expressed using Eqs. (1) and (2).

$$Nd^{3+} \quad + \quad 3\,e^- \quad \rightarrow \quad Nd \qquad (3)$$
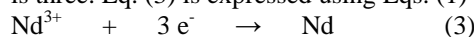
The electrolysis was performed by applying potential at -3.0 V vs. $Cl_2|Cl^-$, which the reduction of Nd^{3+} to Nd^{2+} preceded. After 15 hours for the electrolysis, electric charge measured in the electrolysis was 95% of that calculated based on Fig. 1 by using number of electron, Faraday constant and number of mole. Nd weight remained and dissolving in the melt was measured by ICP-AES to be 7% of the total weight of Nd used in the electrolysis. It was found that 93% of Nd used in the electrolysis formed undissolving metallic fog and reacted with quartz crucible. This result indicated that equilibrium constant of the disproportionation as Eq. (2) is large enough to proceed almost quantitatively (5×10^3 in LiCl-KCl eutectic at 770 K).
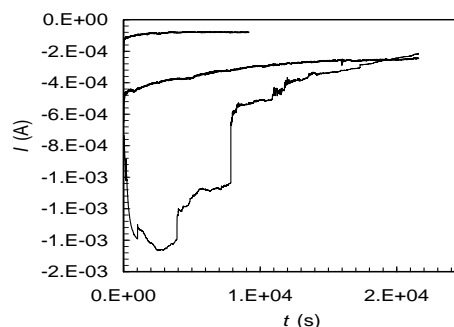

Fig. 1. Current vs. time curve during controlled potential electrolysis by applying -3.0 V vs. $Cl_2|Cl^-$ for three times.

When the electrolysis was performed at -3.3 V vs. $Cl_2|Cl^-$ instead of -3.0 V vs. $Cl_2|Cl^-$, which the Nd^{3+} was directly reduced to form metallic Nd, black deposition on the working electrode as well as black metallic fog in the melt was observed. It was found that metallic Nd fog can be formed through Eq. (1) and (2) as well as Eq.(3).

REFERENCES:
[1] J.P. Ackerman, J.L. Settle, J. Alloys. Comp. **177** (1991) 129.
[2] H. Yamana, B.G. Park, O. Shirai, T. Fujii, A. Uehara, H. Moriyama, J. Alloys Comp.**66** (2006) 408–412.
[3] H. Hayashi, M. Akabori, T. Ogawa, K. Minato, Z. Naturforsch. 59a, (2004) 705.

Chemical Separation of TRU Elements and Fission Products and Their Isotopic Fractionations in the Separation Process

T. Fujii, S. Fukutani, H. Yamana,

Research Reactor Institute, Kyoto University

INTRODUCTION: Hydrate melts (fused hydrated salts) are known as extremely highly concentrated electrolytes. Because of the limited amount of water, the water activity is as small as that of concentrated HNO_3. Extraction of some *f*-elements by TBP from hydrate melts has been performed (see references in [1]). We have interests in the system with calcium nitrate hydrate melts, $Ca(NO_3)_2 \cdot RH_2O$, with water content R less than about 6. In the present study, we investigated the chemical behavior of uranium in $Ca(NO_3)_2 \cdot RH_2O$ by Raman spectrometry.

EXPERIMENTAL: $UO_2(NO_3)_2 \cdot 6H_2O$ was used as uranium nitrate. $Ca(NO_3)_2 \cdot RH_2O$ (R = 4.0 or 8.0) containing ~0.01 M U were prepared. 1 M HNO_3 solution containing the same amount of U was also prepared. 0.4 mL of each solution was transferred into a quartz cell having a 2 mm light path, and this cell was sealed. The Raman scattering was collected at 90° to the incident beam. Raman spectra were obtained by an excitation using the 514.5 nm of an Ar^+ laser (NEC, GLS3280 and GLG 3280) and recorded by a JASCO NR-1100 spectrophotometer at 0.2 cm^{-1} intervals and 120 cm^{-1}/min scanning rate. The laser power at the sample was 400 mW.

RESULTS: The ν_4 vibration of NO_3^- showed Raman shifts in 700-750 cm^{-1} region. The lower frequency vibration around 720 cm^{-1} is known as the vibration of free NO_3^- which is hydrated, and higher one around 740 cm^{-1} the vibration of bound NO_3^- coordinated to cations [2,3]. At high dilution, only lower frequency is observed. The Raman intensity of the higher frequency vibration increases with the decrease of the water content. The shoulder of this frequency can be seen in Fig. 1.

Raman shift of the ν_1 vibration of UO_2^{2+} in nitrate media has been reported to be about 869-873 cm^{-1} (see references in [2]). As shown in Fig. 1, $Ca(NO_3)_2 \cdot 4H_2O$ system shows the ν_1 frequency to be 873 cm^{-1}. The ν_1 symmetric vibrational frequency of UO_2^{2+} is known to decrease with complexation. If nitrate ion coordinates to uranyl ion stronger with the decrease of the water content, a change in Raman shift can possibly be observed. For $Ca(NO_3)_2 \cdot 4H_2O$, $Ca(NO_3)_2 \cdot 8H_2O$, and 1 M HNO_3 systems, the Raman shifts show the same frequency. This indicates that the coordination of nitrate ion less affects the polarizability of U=O bond.
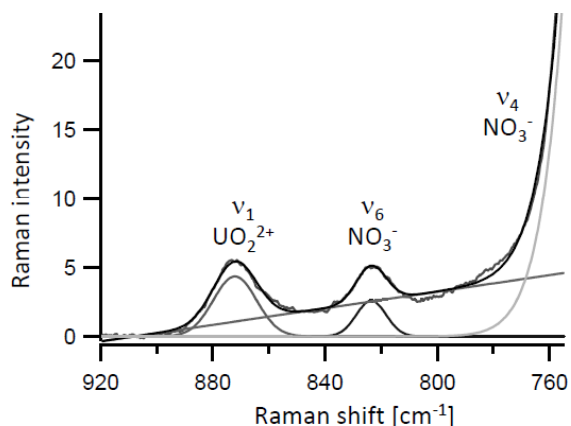

Fig. 1. Raman spectrum of U in a calcium nitrate hydrate melt, $Ca(NO_3)_2 \cdot 4H_2O$.

In our previous study [4], we investigated the chemical behavior of neptunium (^{237}Np) in $Ca(NO_3)_2 \cdot RH_2O$ by Raman spectrometry. Neptunyl ions in $Ca(NO_3)_2 \cdot 4H_2O$ showed a vibrational frequency at 854 cm^{-1}. This would be attributable to the ν_1 frequency of NpO_2^{2+}, nevertheless the frequency was smaller than that found in the 1 M HNO_3 system (859.4 cm^{-1}).

A sharp peak was observed for UO_2^{2+} in 1 M HNO_3, while the sharpness disappeared in $Ca(NO_3)_2 \cdot 8H_2O$ and then in $Ca(NO_3)_2 \cdot 4H_2O$. This may be due to a perturbation of the ν_1 vibration of UO_2^{2+} by co-existed Ca^{2+} and NO_3^- in hydrate melts [2].

REFERENCES:
[1] T. Fujii *et al.*, IOP Conf. Ser. Mater.: Sci. Eng., **9** (2010) 012061(7 pages).
    J. Nucl. Sci. Technol., **32** (1995) 1230-1235.
[2] T. Fujii *et al.*, J. Nucl. Sci. Technol., **suppl. 3** (2002) 336.
[3] H. Kanno and J. Hiraishi, J. Phys. Chem., **88** (1984) 2787-2792.
[4] T. Fujii *et al.*, *KURRI Progress Report 2009* (2010) 115-115.

        Complexation of Thorium with Humic Substances

T. Sasaki, S. Aoyama, H. Yoshida, H. Moriyama[1], T. Fujii[1] and H. Yamana[1]

Department of Nuclear Engineering, Kyoto University
[1]Research Reactor Institute, Kyoto University

INTRODUCTION: Organic substances may greatly affect the speciation and solubility of tetravalent metal ions in deep groundwater, depending on the parameters such as complex formation constants, pH, the ionic strength, the organic ligand-to-metal concentration ratio, aging time, and so on. The thermodynamic stability of the chemical species in aqueous solution varies from the nature of ligand. In order to estimate the contribution of each parameter to the apparent solubility, reliable thermodynamic data in the complexation of M(IV) with anionic ligands such as hydrolysis constants, complex formation constants, and solubility products have been required in the safety assessment of the geological disposal. In the present study, we investigate the formation constant of tetravalent actinide ions, Th, with humic substance by using a solvent extraction method with a trace amount of metal ion.

EXPERIMENTAL: Due to the heterogeneous chemical nature of humic substances, it cannot be clearly defined the number of functional groups per a molecule and the molecular weight. Therefore, by analogy with Langmuir's adsorption isotherm, the apparent formation constant β_{app} is defined as follows; $\beta_{app} = [ML]/([M^{4+}][R^-])$, where $[M^{4+}]$ and $[ML]$ are the concentrations of free metal ion and bound one with humic acid L, and $[R^-]$ is the concentration of the dissociated functional group. Especially for the tetravalent metal ions, however, the hydrolysis reaction in the aqueous phase may be indispensable. In the recent solubility study, Kobayashi et al suggested the presence of the ternary $Th(OH)_2(L)^0$ as the solubility-limiting solid phase, where L was the dicarboxylic acids, while the aqueous species was assumed to be the binary complex $Th(L)_p$ instead of $Th(OH)_n(L)_p$ for the better convergence of the solubility fitting analysis [1]. However, it may not be easy to guess the exact predominant species because of the heterogeneous binding sites of humic substance. At the present stage, therefore, the number of hydroxide ions coordinated to the tetravalent actinide ion would be assumed. Similarly, the formation constant in the presence of the humic acid is expressed by the binary or ternary complex depending on the definition of the species,

$$\beta_{app} = \frac{[M(OH)_qL]}{[M^{4+}][OH]^q[R^-]},$$

where q=1 assumed in the present study. The formation constants were determined by the solvent extraction method which was conducted in a similar manner as that described in the previous study [2]. A sequence of the forward-back extraction system has favorable features to minimize the formation of polynuclear hydrolysis species. Since the mass balance of Th at pHc >3 was more than

90% in the back-extraction, no major unexpected reactions such as adsorption of colloids on the polypropylene vessel wall and precipitation at the liquid-liquid interface were observed. Therefore, the presence of the adsorbed metal ion was ignored in the equilibrium analysis, and the distribution coefficient of Th was calculated by $D = [M]_o/([M]_{ini}-[M]_o)$. From the difference of the distribution ratio between in the presence (D) and absence (D_0) of humic substances,

$$\log\left(\frac{D_o}{D}\right) = \log\left(\frac{1+\sum\beta_{OH,p}[OH^-]^p + \beta_{app,q}[OH^-]^q[R^-]}{1+\sum\beta_{OH,p}[OH^-]^p}\right)$$

When $A = 1+\sum\beta_{OH,p}[OH]_p$,
$$\log D = \log D_o - \log(A + \beta_{app,q}[OH^-]^q[R^-]) + \log A.$$

RESULTS: The tetravalent metal ion complexed with TTA extractants is back-extracted into aqueous phase by complexing with humic acid. The constant D values at the different concentration of humic acid suggest that six hours are sufficient to achieve the equilibrium, that is, the complexation of Th ions with the functional groups of humic acid.

The log β_{app} values of Th(OH)L are more than 20 and increased with an increase of pH as shown in **Fig. 1**. It is noted that the values for the humic substances (HA1 and HA2) in the higher $\log C_R\alpha$ region are different, probably due to the property of functional sites.
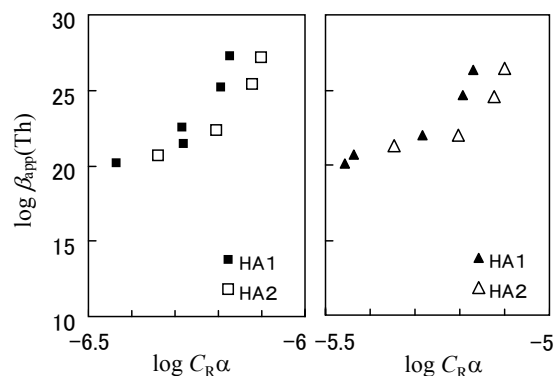

Fig. 1. $C_R\alpha$ dependence on log β_{app} of Th(IV)-OH-humic acid ternary complexes at $I = 0.1$ M and 25°C.
(left) ■; $C_M=2\times10^{-9}\sim9\times10^{-9}$ M, $C_R=1\times10^{-6}$ eq/dm³, □; $C_M=5\times10^{-9}\sim1\times10^{-8}$ M, $C_R=1\times10^{-6}$ eq/dm³,
(right) ▲; $C_M=1\times10^{-8}\sim7\times10^{-8}$ M, $C_R=1\times10^{-5}$ eq/dm³, △; $C_M=1\times10^{-8}\sim6\times10^{-8}$ M, $C_R=1\times10^{-5}$ eq/dm³.

REFERENCES:
[1] Kobayashi, T., Sasaki, T., Takagi, I., Moriyama, H., *J. Nucl. Sci. Technol.* (2011) in press.
[2] Sasaki, T., Kobayashi, T., Takagi, I., Moriyama, H., Fujiwara, A., Kulyako, Y. M., Perevalov, S. A., Myasoedov, B. F., *Radiochim. Acta* **97**, (2009) 193.

PR1-6   Estimation of UO_2^{2+}/UO_2^+ Redox Potential in Alkaline Molybdate Melt

T. Nagai, A. Uehara[1], T. Fujii[1], M. Myochin and
H. Yamana[1]

Japan Atomic Energy Agency (JAEA)
[1]*Research Reactor Institute, Kyoto University*

INTRODUCTION: A pyrochemical process by using alkaline molybdate melts has been studied as a promising reprocessing process of spent nuclear oxide fuels. In our previous study [1,2], it was confirmed by the absorption spectrophotometry in Li_2MoO_4–Na_2MoO_4 eutectic melt that the uranyl ions existed stably as the penta-valent, UO_2^+, and UO_2^+ was easily oxidized to the hexa-valent, UO_2^{2+}, by purging oxygen gas. And the UO_2^{2+}/UO_2^+ redox reaction was observed by the cyclic voltammetry. However, it was difficult to determine the UO_2^{2+}/UO_2^+ redox potential, because the reduction potential of UO_2^{2+} was close to the deposition potential of molybdenum compounds. In this work, this redox potential was estimated by using the spectrophotometric technique.

EXPERIMENAL: All operations were carried out in a glove box filled with dry Ar gas. Anhydrous Li_2MoO_4 and Na_2MoO_4 purchased from Kojundo Chemical Lab. Co., Ltd. were more than 99 % in purity, and processed by the vacuum drying at 150 °C before use. The Li_2MoO_4–Na_2MoO_4 eutectic was prepared by melting the mixed anhydrous reagents at 750 °C. The UO_2^+ source material containing UO_2^+ was obtained by dissolving the UO_2 powder into the eutectic melt without other treatments. And the UO_2^{2+} source material containing UO_2^{2+} was oxidized the UO_2^+ source material melt by purging O_2.

In the measurement, the prepared eutectic was put into the quartz tube which had a welded optical measurement cell at the bottom of tube. Then they were heated to 550 °C. After measuring the background absorption spectrum of the pure melt, a portion of the UO_2^+ source material was added into the melt and the spectrum of UO_2^+ was measured. And working and reference electrodes were inserted into the cell and the equilibrium potential, *E*, was measured. The working electrode was used a platinum wire, and the reference electrode utilized was composed of a Pyrex tube with 12.17 mol% MoO_3 in the eutectic and a platinum wire. After this potential measurement, a small amount of the UO_2^{2+} source material was added into the melt, and the spectrum and potential were measured sequentially in the presence of UO_2^{2+} and UO_2^+. These operations of the UO_2^{2+} source material addition and measurements were repeated until the concentration of UO_2^{2+} increased to twice that of UO_2^+.

RESULTS: Figure 1 shows the observed absorption spectra of UO_2^+ with repeating the addition of the UO_2^{2+} source material. The absorption peak at 7000 cm^{-1} cor-

responded to UO_2^+, and this peak did not grow so much with an increase in the added amount of the UO_2^{2+} source material. However, a small amount of UO_2^{2+} in the source material was reduced to UO_2^+ after the dissolution, because UO_2^+ was stable in the Li_2MoO_4–Na_2MoO_4 eutectic melt. In the wavenumber range showed in Fig.1, UO_2^{2+} does not have any absorption band.

To estimate the UO_2^{2+}/UO_2^+ redox potential by applying the Nernst equation (1), the concentrations of UO_2^{2+} and UO_2^+ were calculated from the observed absorption spectra and their molar absorptivities. The concentration of UO_2^+ was obtained from the absorption peak and its absorptivity at 7000cm^{-1}, and that of UO_2^{2+} was a difference from total uranyl and UO_2^+. Fig. 2 shows the relation between the logarithm concentration ratio, $ln[UO_2^{2+}]/[UO_2^+]$, to the *E* in the melt. From Eq.(1), *E* at $ln[UO_2^{2+}]/[UO_2^+] = 0$ was the redox potential, *E*°, and it was determined to *E*°=0.277±0.010 V (*vs.* reference electrode). This redox reaction is one-electron exchange, and the slope showed in Fig.2 is 13.44. This value is close to the theoretical value of 14.10.

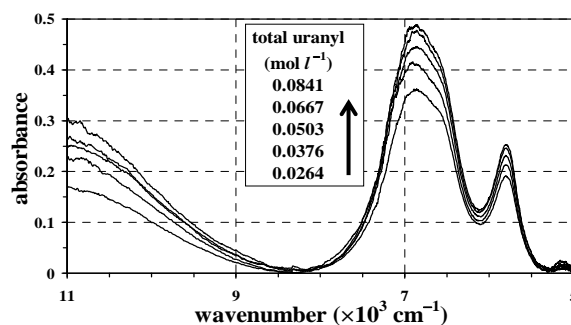$$E = E°(UO_2^{2+}/UO_2^+) + (RT/F) \, ln[UO_2^{2+}/UO_2^+] \quad (1)$$

Fig.1.   Absorption spectra of UO_2^+ and adding UO_2^{2+} in Li_2MoO_4–Na_2MoO_4 at 550 °C.
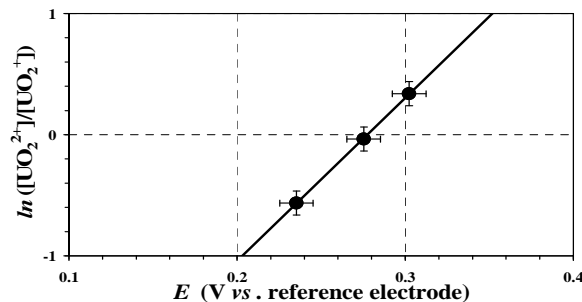
Fig.2.   Relation of concentration ratio, $ln[UO_2^{2+}]/[UO_2^+]$, to potential, *E*, in Li_2MoO_4–Na_2MoO_4 at 550 °C.

REFERENCES:
[1] T. Nagai, M. Fukushima,
    A. Uehara, T. Fujii, M. Myochin, H. Yamana, *2008FY KURRI progress report*, PR4-9 (2009).
[2] T. Nagai, M. Fukushima, A. Uehara, T. Fujii,
    M. Myochin, H. Yamana, *2009FY KURRI progress report*, PR4-7 (2010).

PR1-7 Chronopotentiometric Study on Anodic Behavior of U-Zr Alloy in LiCl-KCl Melt at 773 K

M. Iizuka, T. Fujii[1], A. Uehara[1] and H. Yamana[1]

Central Research Institute of Electric Power Industry
[1]Research Reactor Institute, Kyoto University

INTRODUCTION: In the multi diffusion layer anode model of U-Zr alloy, which is developed for analysis of the molten salt electrorefining process for the spent metallic fast reactor fuel, (a) the solubility of UCl_3 in LiCl-KCl melt, and (b) the diffusion coefficient of actinide ions in the porous zirconium layer [2] formed at the surface of the spent metallic fuel by selective dissolution of the actinides, have great influence on the calculation results [1]. In this study, a possibility to apply chronopotentiometry to determination of these numbers was preparatorily investigated.

THEORY: During the chronopotentiometry measurement, a constant anodic current is imposed to U-Zr alloy electrode in LiCl-KCl melt, resulting in the preferential dissolution of uranium due to its lower standard redox potential than that of zirconium. Since the rate of uranium supply from the U-Zr alloy is essentially unlimited during the short term measurement, the transition from $U^0 = U^{3+} + e^-$ to $Zr^0 = Zr^{4+} + 4e^-$ in the chronopotentiogram is caused by the limitation of U^{3+} diffusion in the melt. In the practical situation, this limitation is determined by the highest possible concentration of U^{3+} at the surface of the electrode, i.e. the solubility of UCl_3 in LiCl-KCl melt. Then, the relation between the transition time and the other parameters is described using the following Sand's equation ;

$$\frac{I\tau^{1/2}}{Sol_{UCl_3} - C^0_{UCl_3}} = \frac{3FAD_{UCl_3}^{1/2}\pi^{1/2}}{2} \qquad (1)$$

where,

I : applied anodic current (A)
τ : transition time (s)
Sol_{UCl_3} : solubility of UCl_3 in LiCl-KCl (mol/cm^3)
$C^0_{UCl_3}$: initial concentration of UCl_3 in LiCl-KCl (mol/cm^3)
F : Faraday's constant (96485 C/equiv.)
A : surface area of U-Zr alloy electrode (cm^2)
D_{UCl_3} : diffusion coefficient of U^{3+} in LiCl-KCl (cm^2/s)

EXPERIMENTS: The U-9 wt% Zr alloy rod was fabricated by injection casting [3]. This rod was cut into around 5mm in length and embedded in a stainless steel holder to limit the exposed area to one polished flat side. The chronopotentiograms were measured in LiCl-KCl-UCl_3 (1 wt%-U) at 773 K before and after the selective anodic dissolution of uranium at controlled potential.

RESULTS: The first group of the chronopotentiometric measurements was carried out using U-Zr alloys before the total anodic charge passed through their surface amounted to about 150 C/cm^2. Since the porous Zr layer of a significant thickness does not form under this condition, it is proper to consider that the D_{UCl_3} calculated from the transition time observed in the first group of measurements corresponds to the diffusion coefficient in the bulk LiCl-KCl. Based on this consideration, 0.00359 mol/cm^3 was chosen as Sol_{UCl_3} in equation (1), the solubility of UCl_3 in LiCl-KCl, to adjust the average D_{UCl_3} value evaluated from the measured chronopotentiograms to 1.0×10^{-5} cm^2/s, at which most of the literatures are in agreement. The solubility value evaluated in this study was about 15 % larger than that mentioned in a U.S. patent description [4].

The second group of the chronopotentiograms was measured after the anodic dissolution of more than 2500 C/cm^2 at controlled potential for selective oxidation of uranium. Since the porous Zr layer of a sufficient thickness was considered to form by this process, it is reasonable to regard the D_{UCl_3} values evaluated from the result of this group of measurements as those in LiCl-KCl melt infiltrating into the porous Zr layer. Although these data is largely dispersed, there can be seen its positive correlation with the interval after the just prior measurement (Fig. 1). This behavior probably comes from the UCl_3 concentration gradient in the porous Zr layer that remains for a long period of time particularly after this layer has grown thicker. Then, the correct D_{UCl_3} in this layer should be evaluated after sufficient relaxation of the concentration gradient. In this study, the first measurement after a long interval (280 min.) should give the most appropriate value, 7.3×10^{-6} cm^2/s. D_{UCl_3} in the porous Zr layer assumed in the anode model (7.0×10^{-6} cm^2/s [1]) by fitting between the calculated and actual electrorefining results closely agrees with the evaluated value in this study.
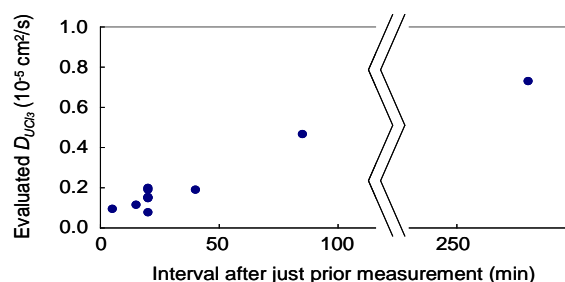

Fig. 1 Relationship between Evaluated D_{UCl_3} value and interval after just prior measurement

REFERENCES:
[1] M.Iizuka *et al.*, J. Nucl.Sci.Technol., **47** (2010) 1140.
[2] M.Iizuka *et al.*, J. Nucl.Sci.Technol., **46** (2009) 699.
[3] T.Ogata *et al.*, Proc. Global 2007(2007).
[4] J.Willit, U.S. patent 7267754 (2007).

PR1-8   Extraction Behavior of Tungsten from Hydrochloric Acid Solution as Homologue of Element 106, Seaborgium

K. Ooe, T. Yokokita, Y. Komori, R. Takayama, Y. Kasamatsu, T. Yoshimura, N. Takahashi, H. Kikunaga[1], H. Haba[2], Y. Kudou[2], K. Takamiya[3] and A. Shinohara

Graduate School of Science, Osaka University
[1]*Research Center for Electron Photon Science, Tohoku University*
[2]*Nishina Center for Accelerator-Based Science, RIKEN*
[3]*Research Reactor Institute, Kyoto University*

INTRODUCTION: Seaborgium (element 106, Sg) is an artificial radioactive element belonging to the group 6. Because of the low production rate and the short half-life of Sg, it is very difficult to realize the chemical studies of Sg and little is known about the chemical properties. In this work, solvent extraction behavior of tungsten (W), which is a lighter homologue of Sg, from hydrochloric acid solution was investigated as a preliminary study for Sg. Extractants used in this study were Aliquat 336 which extract anionic species in an aqueous solution.

EXPERIMENTS: The tungsten isotope, ^{187}W ($T_{1/2}$ = 27.32 h) was produced by irradiation of Na_2WO_4 with neutrons in the pneumatic irradiation facility (Pn-2) of Kyoto University Reactor (KUR). The other isotope, ^{173}W ($T_{1/2}$ = 7.6 min) was also produced in the $^{nat}Gd(^{22}Ne,xn)^{173}$W reaction using the RIKEN K70 AVF cyclotron. In the experiment at RIKEN, reaction products recoiling out of the target were transported to the chemistry laboratory by a He/KCl gas-jet transport system. The transported products were deposited on a polyester or Naflon sheet for 5 min. The radioisotopes of ^{187}W and ^{173}W were separately dissolved in 200 μL of hydrochloric acid (HCl) solution. The aqueous phase was mixed with an equal volume of the Aliquat 336-chloroform solution. The mixture was shaken for 3 min. After centrifuging, 160 μL aliquots of the aqueous and organic phases were taken separately into polypropylene tubes and were then subjected to the γ-ray spectrometry using Ge detectors. Distribution ratios (D) were obtained from the radioactivities in the aqueous and organic phases.

RESULTS: Figure 1 shows the distribution ratios of W as a function of hydrochloric acid concentration [HCl]. The D values of W rise with the increase of [HCl], suggesting that the anionic chloride complexes of W are formed. It has been reported that the extracted species of W is $WO_2Cl_3^-$ or $WO_2Cl_4^{2-}$ [1,2].

The D values of W were also investigated in 10.8 M HCl solution as a function of Aliquat 336 concentration. The result is shown in Fig. 2. The plots of log D vs. log

Aliquat 336 concentration give a linear correlation with a slope of 1.14 ± 0.02. This indicates that the net charge of W chloride complex is -1. Therefore, the extracted species of W would be $WO_2Cl_3^-$.

In the present study, from the extraction behavior of W, the chemical species of W was able to be deduced. Based on these results, we will determine the experimental conditions of the Sg experiment and clarify the chemical properties of Sg.
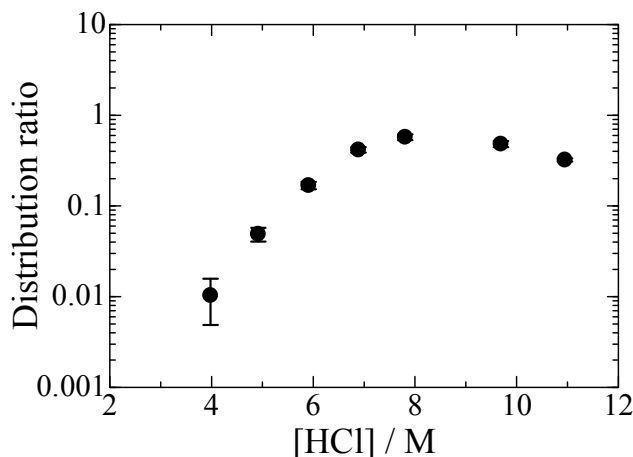

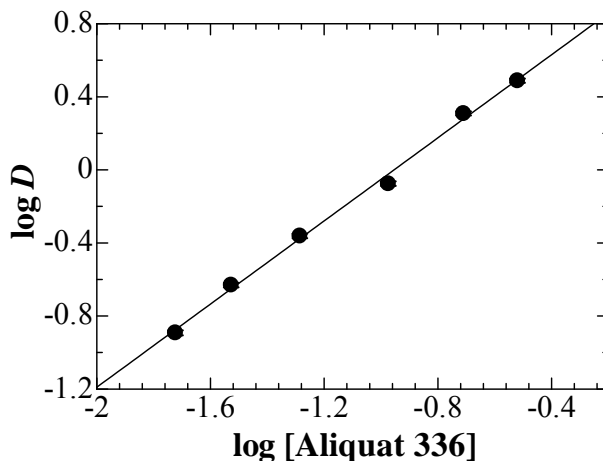Fig. 1. Extraction of W from HCl solution with 0.05 M Aliquat 336-chloroform solution.

Fig. 2. Distribution ratios of W as a function of Aliquat 336 concentration. The concentration of HCl was 10.8 ± 0.1 M.

REFERENCES:
[1] K. A. Kraus *et al.*, J. Am. Chem. Soc., **77** (1955) 3972-3977.
[2] T. Sato and K. Sato, Hydrometallurgy., **37**(1995) 253-266.

PR1-9   Electrochemical Study on Uranyl(VI) Complexes in Ionic Liquid Media to Find Stable Uranyl(V)

T. Ogura and Y. Ikeda

Research Laboratory for Nuclear Reactors, Tokyo Institute of Technology

INTRODUCTION: Most of actinoid(V) and (VI) complexes contain actinyl ions (AnO_2^{n+}, An = U, Np, Pu, Am; n = 1 or 2). However, only a limited data on properties of uranyl(V) species has been available, because the uranyl(V) species are unstable in solutions due to disproportionation [1]. Hence, we have devoted to discover the stable uranyl(V) species in liquid state. As a result, we found some stable uranyl(V) complexes, $[UO_2(CO_3)_3]^{5-}$ in aqueous solution, $[UO_2(dbm)_2DMSO]^-$, $[UO_2(saloph)DMSO]^-$, and $[UO_2(saldien)]^-$ in DMSO (dbm = dibenzoylmethanate, saloph = *N,N'*-disalicylidene-*o*-phenylenediaminate, saldien = *N,N*-disalicylidenediethylenetriaminate, DMSO = dimethyl sulfoxide) [2]. From the studies on properties of these complexes, it was clarified that the U=O bond distance becomes long with the reduction from U(VI) to U(V), that the uranyl(V) complexes have characteristic absorption bands around 650, 750, 900, 1450, 1850 nm, and that uranyl(V) is more labile than uranyl(VI). Furthermore, it has been known that uranyl(V) ion is formed in LiCl-$MgCl_2$ molten salt [3].

From these studies, it was proposed that requirements for the formation of stable U(V) complexes in solutions are as follows; to prevent the formation of the dimeric complex (oxo-bridged cation-cation complex), to use the bulky ligands to protect effectively the formation of cation-cation complex, to use the ligands which can strongly coordinate to the equatorial plane of uranyl(V), *e.g.*, pyridine, dmso, and to be fully coordinated by Cl^- such as $[UO_2Cl_4]^{2-}$ formed in chloride molten salt.

In the present study, we have examined the chemical structure and electrochemical behavior of uranyl(VI) species, $(EMI)_2UO_2Cl_4$, in the mixture of EMICl and EMIBF$_4$ (EMI = 1-ethyl-3-methylimidazoliun)

EXPERIMENTS: Cyclic voltammograms of the mixture of EMICl and EMIBF$_4$ (EMI = 1-ethyl-3-methyl imidazolium) dissolving $[EMI]_2[UO_2Cl_4]$ were measured using an electrochemical analyzer (BAS, ALS model 660B) in a glove box under an Ar atmosphere at 25 ± 1 °C. A Pt electrode(BAS, diameter = 1.6 mm), a Pt wire, an Ag/Ag$^+$ electrode (BAS, RE-5B) were used as a working, a counter, and a reference electrodes, respectively. All potentials reported here are *vs.* Fc/Fc$^+$.

RESULTS: Uranyl species were found to exist as $[UO_2Cl_4]^{2-}$ in the mixture of EMICl and EMIBF$_4$ (mole fraction = 1 : 1). The cyclic voltamograms (Figure) measured at various scan rates ($v = 50 - 300$ mV/s) show one redox couple around -1.0 V *vs.* Fc/Fc$^+$, that the values of ($E_{pc} + E_{pa}$)/2 (E_{pc} and E_{pa} are peak potentials for cathodic and anodic peaks, respectively) are constant (-0.989 V *vs.* Fc/Fc$^+$) regardless of the scan rates, and that the plot of i_{pc} (the peak currents of cathodic peaks) against $v^{1/2}$ gives a linear relationship with slope of 8.21. These results suggest that the electrochemical reaction of $[UO_2Cl_4]^{2-}$ reduced to $[UO_2Cl_4]^{3-}$ almost reversibly and that the resulting $[UO_2Cl_4]^{3-}$ is relatively stable.
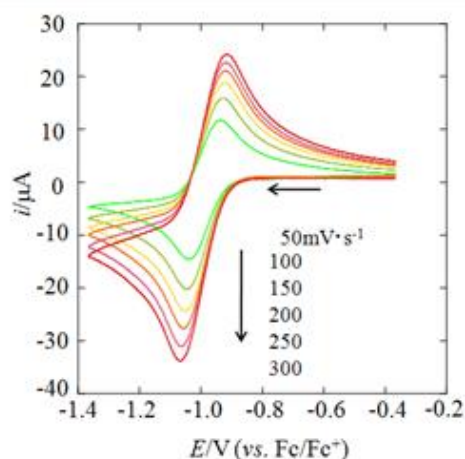

Fig.1. Cyclic valtammograms of mixture of EMICl and EMIBF$_4$ dissolving $[EMI]_2[UO_2Cl_4]$ (6.06×10^{-2} M).

REFERENCES:
[1] a) T.W. Newton and F.B. Baker, *Inorg. Chem.*, **4**, (1965) 1166.
[2] a) K. Mizuoka, S.-Y. Kim, M. Hasegawa, T. Hoshi, G. Uchiyama, and Y. Ikeda, *Inorg. Chem.*, **42** (2003) 1031.
b) K. Mizuoka, S. Tsushima, M. Hasegawa, T. Hoshi, and Y. Ikeda, *Inorg. Chem.*, **44** (2005) 6211.
c) K. Takao, M. Kato, S. Takao, A. Nagasawa, G. Bernhard, C. Hennig, and Y. Ikeda, Inorg. Chem., **49** (2010) 2349.
[4] M.D. Adams, D.A. Wenz, and R.K. Steunenberg, *J. Phys. Chem.* **67** (1963) 1939.